Hindawi
Advances in Civil Engineering
Volume 2019, Article ID 8167651, 15 pages
https://doi.org/10.1155/2019/8167651

Research Article

Coupled Effect of Water Temperature and Cyclic Wetting and Drying on Dynamic Mechanical Characteristics of Sandstone

Pu Yuan[1,2,3] **Ning-Ning Wei**[1] **Qin-Yong Ma**[1,2,3] **and Ju-Cai Chang**[2,4]

[1]*School of Civil Engineering and Architecture, Anhui University of Science and Technology, Huainan 232001, China*
[2]*State Key Laboratory of Mining Response and Disaster Prevention and Control in Deep Coal Mines, Anhui University of Science and Technology, Huainan 232001, China*
[3]*Engineering Research Center of Underground Mine Construction, Ministry of Education, Anhui University of Science and Technology, Huainan 232001, China*
[4]*School of Energy and Safety, Anhui University of Science and Technology, Huainan 232001, China*

Correspondence should be addressed to Pu Yuan; puy2012@126.com

Received 11 June 2019; Revised 14 August 2019; Accepted 9 September 2019; Published 30 September 2019

Academic Editor: Hui Yao

Considering the periodical moisture variation in deep rock masses, cyclic wetting and drying under high geothermal condition is a vital issue for the safety and stability of deep rock engineering. To investigate the coupled effect of water temperature and cyclic wetting and drying on dynamic mechanical characteristics of sandstone, dynamic uniaxial compressive tests were carried out under the same loading condition for sandstone specimens subjected to cyclic wetting and drying treatment. When the temperature was 60°C in both wetting and drying processes, cyclic wetting and drying treatment presents a detrimental effect on the tested sandstone. Both physical and dynamic uniaxial compressive characteristics deteriorate in an exponential function with the increase of wetting and drying cycles. Based on SEM image analyses, the initiation and propagation of microcracks is mainly the result of cyclic loading and unloading of tensile stresses induced by water absorption and desorption of kaolinite within sandstone during cyclic wetting and drying treatment. After 15 cycles of wetting and drying, the deterioration of both physical and dynamic uniaxial compressive characteristics first increase then decrease with water temperature in wetting process elevating from 20°C to 98°C. SEM images indicate that more microcracks generate when water temperatures increase from 20°C to 60°C, while the micromorphology is changed and fewer microcracks display due to kaolinite mobilization when water temperature increases from 60°C to 98°C. The threshold value for the effect of water temperature on cyclic wetting and drying is found to be about 60°C for the tested sandstone.

1. Introduction

In rock engineering, the deterioration of physical and mechanical properties of rock is generally associated with water weathering [1], such as wetting and drying cycles [2], freezing and thawing cycles [3], and heating and cooling cycles [4]. The damage and mechanical properties of rock induced by water weathering is a vital issue for the stability of rock engineering, particularly the stability of rock slopes and underground caverns in hydraulic engineering [5, 6]. It even leads to natural geologic hazards in underground rock engineering with respect to strong corrosion of groundwater flow [7], especially in mining engineering [8, 9]. Due to periodical moisture variation induced by a seasonal change of groundwater level, rainfall, and other reasons, water weathering process of rock is accelerated by cyclic wetting and drying [10, 11]. The influence of cyclic wetting and drying on physical and mechanical properties of rock has been researched recently.

As for physical properties, the deterioration induced by cyclic wetting and drying can be evaluated by the variation of bulk density, water content, porosity, P-wave velocity, slake durability index, etc. Pardini et al. [12] studied the variation of surface roughness, bulk density, and porosity of smectitic mudrock subjected to cyclic wetting and drying treatment and found a little reduction of bulk density and an increase

of porosity after 3 cycles of wetting and drying. Özbek [13] reported that with the increase of wetting and drying cycles, both bulk density and P-wave velocity of ignimbrite decreased, while both water content and effective porosity increased. Gökceoğlu et al. [14] studied the factors affecting the slake durability index of clay-bearing rocks and the influence of wetting and drying cycles on the slake durability index values.

As for mechanical properties, the deterioration induced by cyclic wetting and drying should be investigated in both static and dynamic conditions. However, most of the investigations on deterioration induced by cyclic wetting and drying were focused on static mechanical properties, and limited studies can be found on dynamic mechanical properties. Hale and Shakoor [1] investigated the effect of cyclic wetting and drying on static uniaxial compressive strength of six kinds of sandstone after suffering 50 cycles of wetting and drying, and no obvious correlation was found between uniaxial compressive strength and wetting and drying cycles. Zhao et al. [15] reported that static tensile strength of sandstone with a low clay mineral content was not sensitive to cyclic wetting and drying treatment. However, recent researches indicated that static uniaxial compressive strength and tensile strength decreased remarkably with the increase of wetting and drying cycles [16, 17]. The discrepancy variation of static uniaxial compressive strength and tensile strength is the result of different mineralogical composition and microstructure. Zhang et al. [18] studied the effect of cyclic wetting and drying on shear strength of argillaceous siltstone, and the shear strength of siltstone under same vertical stress decreased with the increase of wetting and drying cycles. By using centrally cracked Brazilian disc specimens, Hua et al. [19] reported that both mode I and mode II fracture toughness of sandstone decreased with the increase of wetting and drying cycles. By conducting uniaxial compressive creep tests siltstone in a step loading way, Ma et al. [10] reported that both axial creep strain and axial steady creep rate increased with the increase of wetting and drying cycles, while instantaneous deformation modulus decreased.

In consideration of extensively blasting operation in rock excavation [20, 21], recent researches referred to the influence of cyclic wetting and drying on dynamic mechanical properties. Du et al. [11] reported that dynamic compressive strength of red-sandstone decreased with the increase of wetting and drying cycles. Yuan and Ma [22] carried out dynamic uniaxial compressive tests for coalmine sandstone subjected to cyclic wetting and drying and reported that dynamic uniaxial compressive strength reduced in a power relationship with wetting and drying cycles. With the help of split Hopkinson pressure bar (SHPB) apparatus, Zhou et al. [23, 24] found that both dynamic compressive strength and tensile strength of fine-grained sandstone decreased with the increase of wetting and drying cycles.

Currently, researches on the influence of cyclic wetting and drying on rock properties hardly involve the temperature effect on cyclic wetting and drying process. In deep underground engineering, the temperature of rock increases at a speed of 30°C/km to 50°C/km with the burial depth. When burial depth was beyond 1000 m, the temperature was over 40°C, sometimes even exceeding 60°C [25]. Some researches indicated that water weathering effect was affected by water temperature [26, 27]. As rock engineering disasters are closely related with dynamic rock failure under stress pulses or impact loads, the investigation on dynamic mechanical characteristics of sandstone under coupled effect of water temperature and cyclic wetting and drying is meaningful to the safety and stability of deep rock engineering.

The objectives of this research were to figure out the deterioration of dynamic mechanical characteristics induced by cyclic wetting and drying and the effect of water temperature on cyclic wetting and drying. In this study, dynamic uniaxial compressive tests were carried out for sandstone after cyclic wetting and drying in various water temperatures based on modified SHPB apparatus. Then, dynamic compressive strength, dynamic elastic modulus, average strain rate, fractal dimension, and damage evolution were analyzed to characterize the deterioration induced by cyclic wetting and drying, and the effect of water temperature on the process of cyclic wetting and drying was figured out. In addition, microscopic features of sandstone were also observed by scanning electron microscope (SEM) technique.

2. Cyclic Wetting and Drying Treatment and SHPB Test Validation

2.1. Sandstone Specimen Preparation. Sandstone samples with high petrographical uniformity and no visible geological weakness were extracted from the same place at −848 m level of Guqiaobei Coalmine of Huainan Mining Group in Anhui Province, China. Energy dispersive spectroscopy (EDS) was used to determine chemical elements in the sandstone sample, and the main chemical elements of tested sandstone are O (43.52%), Si (30.66%), Al (17.07%), and K (7.22%). According to X-ray diffraction (XRD) analysis, the main mineral components of tested sandstone are quartz (36.4%), kaolinite (39.4%), feldspar (21.5%), and other minerals (2.7%), which are illustrated in Figure 1.

Static uniaxial compressive tests were carried out by the RMT-150B rock mechanics testing system in a loading rate of 0.01 mm/s. And static uniaxial compressive strength, elastic modulus, and Poisson's ratio are 63.07 MPa, 9.92 GPa, and 0.183, respectively.

In accordance with International Society for Rock Mechanics and Rock Engineering (ISRM) suggested method [28], all sandstone specimens were processed into a short cylinder with a diameter of 50 mm and length of 25 mm. After drilling, cutting, and grinding processes, end-face roughness of the sandstone specimen was less than 0.02 mm and end face perpendicular to its axis was within 0.025 mm for dynamic uniaxial compressive tests [28, 29].

2.2. Procedure of Cyclic Wetting and Drying Treatment. Cyclic wetting and drying is a significant issue in rock engineering. Generally, a single cycle of wetting and drying consists of two steps, drying process and wetting process. However, the treatment methods used for wetting process

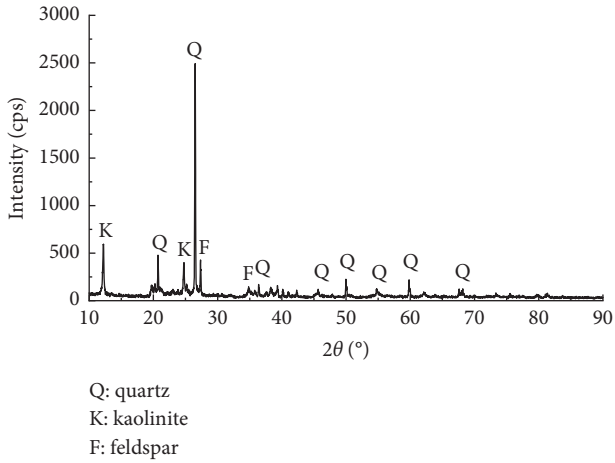

Figure 1: XRD spectrum of tested sandstone.

and drying process can be quite different. Commonly used wetting treatment methods were immersed in water [1, 22, 23, 30] or immersed in water under vacuum condition [31, 32]. The common drying treatment methods were dried in air condition [23, 33] or dried in an oven [1, 22, 32]. Considering the influence of water temperature on the process of cyclic wetting and drying, a thermostatic water bath was used for wetting process. As illustrated in Figure 2, sandstone specimens were dried in an oven during drying process and immersed in a distilled water bath during wetting process in this study.

It is seen from Figure 2 that sandstone specimens were first put into a drying oven at 110°C for 24 h and then immersed in a water bath at designed temperature for 24 h. In the first cycle of wetting and drying treatment, the temperature of the drying oven was set as 110°C to measure the mass of oven-dried sandstone specimens, and then the temperature of drying oven was set as 60°C for the following cycles of wetting and drying treatment. In order to ensure sandstone specimen absorbing water comprehensively, glass rods with a diameter of 6 mm and interval of about 25 mm were put beneath the sandstone specimens as illustrated in Figure 2.

Dynamic uniaxial compressive tests were carried out when wetting and drying cycles achieved 1, 5, 10, 15, and 20 at a water temperature of 60°C in the wetting process. As for 15 cycles of wetting and drying treatment, 5 kinds of water temperatures were accomplished by setting the temperature of the thermostatic water bath as 20°C, 40°C, 60°C, 80°C, and 98°C in the wetting process.

2.3. SHPB Test Procedure and Validation Analyses. As illustrated in Figure 3, dynamic uniaxial compressive tests were carried out by using a modified SHPB apparatus.

Dynamic uniaxial compressive tests were conducted in five steps: (1) aligning elastic bars and keeping striker, input bar, and output bar at the same line axially [34]; (2) mounting strain gauges diametrically on the surface of input bar and output bar [35]; (3) sandwiching sandstone specimen between input bar and output bar and applying lubricant on the contact surfaces; (4) launching the striker and collecting test signals; (5) Gathering the fragments of sandstone specimens.

SHPB technique is based on two fundamental assumptions, one-dimensional stress wave propagation and stress uniformity [28, 36]. For rock-like brittle material, traditional rectangular loading stress wave led to premature failure before stress equilibrium and high signal oscillation due to wave dispersion, which made test results unreliable [37]. With good immunity to premature failure before stress equilibrium, geometric dispersion effect, and Pochhammer-Chree oscillation, half-sine loading stress wave was found to be a suitable, rational, and effective waveform for rock-like materials [28, 37, 38]. Therefore, a cone-shaped striker was used to generate the half-sine loading stress wave in dynamic uniaxial compressive tests [34, 39]. The amplitude and duration of the half-sine loading stress wave were about 192 MPa and 160 μs, respectively.

By comparing the dynamic stresses on both ends of the sandstone specimen, stress equilibrium was checked to validate the dynamic uniaxial compressive tests [40, 41]. Figure 4 presents the acquired incident stress wave $\sigma_I(t)$, reflected stress wave $\sigma_R(t)$, transmitted stress wave $\sigma_T(t)$, sum of incident and reflected stress waves $\sigma_I(t) + \sigma_R(t)$, and dynamic strain of sandstone specimen without cyclic wetting and drying treatment.

As illustrated in Figure 4, the curve of transmitted stress wave almost overlaps with the sum of incident and reflected stress waves, which indicates roughly identical dynamic stresses on both ends of the sandstone specimen. The roughly identical dynamic stresses on the ends of the specimen ensure the assumption of stress uniformity and the reliability of test results.

Clearly from Figure 4, an obvious flat region presents in reflected stress wave. As the strain rate is closely related with the reflected stress wave, the flat region in the reflected stress wave indicates the same variation of the strain rate. With respect to the flat region in the reflected stress wave, an approximate uniform deformation of the sandstone specimen is found in the strain-time curve. Hence, the half-sine loading stress wave gives an approximate constant strain rate deformation in the dynamic uniaxial compressive tests.

According to one-dimensional stress wave theory, the loading stress wave has to propagate several times between two ends of the specimen to attain stress uniformity [42]. In order to evaluate the stress uniformity issue during loading process, a dimensionless stress nonuniformity coefficient $\alpha(t)$ is introduced and defined as the ratio of the absolute value of stress deviation between two ends of the sandstone specimen to their average value [35, 43]:

$$\alpha(t) = \left| \frac{\sigma_T(t) - (\sigma_I(t) + \sigma_R(t))}{(\sigma_T(t) + (\sigma_I(t) + \sigma_R(t)))/2} \right| \times 100\%. \quad (1)$$

As illustrated in Figure 5, the dimensionless stress nonuniformity coefficient attenuates in a serrated fluctuation with the increase of loading time. And the dimensionless stress nonuniformity coefficient attenuates to less than 5% at about 63 μs, which indicates a stress

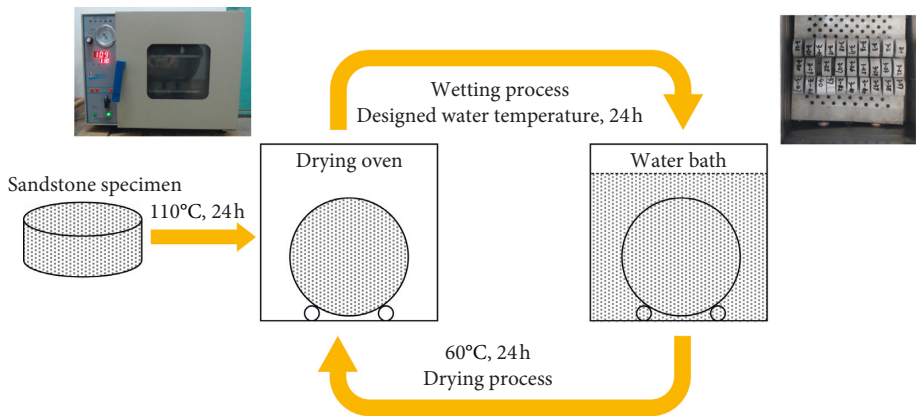

Figure 2: Schematic diagram of cyclic wetting and drying treatment.

Figure 3: SHPB apparatus for dynamic uniaxial compressive tests.

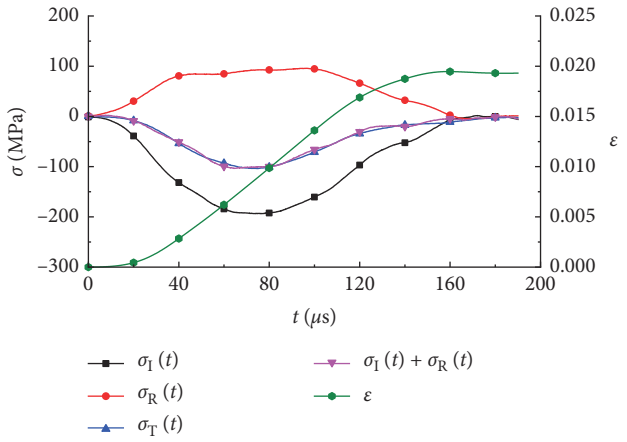

Figure 4: Dynamic stresses and strain in the dynamic uniaxial compressive test.

uniformity state after 63 μs. Therefore, premature failure is eliminated and the stress equilibrium state is achieved before failure in dynamic uniaxial compressive tests.

3. Physical Properties Variation during Cyclic Wetting and Drying Treatment

3.1. Water Content Variation during Cyclic Wetting and Drying Treatment. Water content was calculated by measuring the mass variation of sandstone specimens after different wetting and drying cycles [44, 45]. When

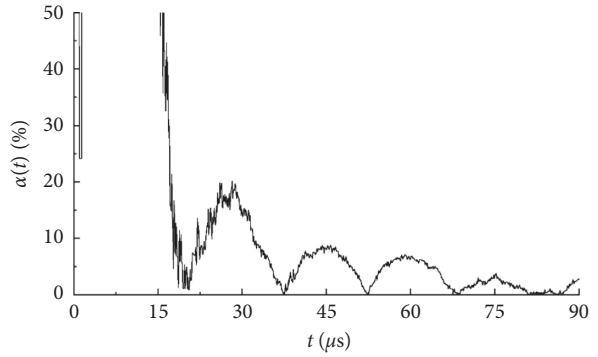

Figure 5: Time history of dimensionless stress nonuniformity coefficient.

measuring the mass of the wet sandstone specimen, water moisture on its surface was wiped by using a filter paper. Water content of the wet sandstone specimen is calculated by using the following equation:

$$w = \frac{M_n - M_s}{M_s} \times 100\%, \quad (2)$$

where w stands for water content of the wet sandstone specimen, M_n is the mass of the wet sandstone specimen after n cycles of wetting and drying treatment, and M_s is the mass of the oven-dried sandstone specimen.

The variation of water content after cyclic wetting and drying treatment is shown in Figure 6.

As illustrated in Figure 6(a), water content of the wet sandstone specimen increases in an exponential function with the increase of wetting and drying cycles. As water filled in open pores and microcracks of the sandstone specimen, an increase in water content indicated more open pores and microcracks in the sandstone specimen after cyclic wetting and drying treatment.

It is seen from Figure 6(b) that water content fluctuates with the increase of water temperature in wetting process. Compared with water content at 20°C, elevating water temperature in wetting process leads to an increase in water content of the sandstone specimen after 15 cycles of wetting and drying treatment, that is to say, water content is

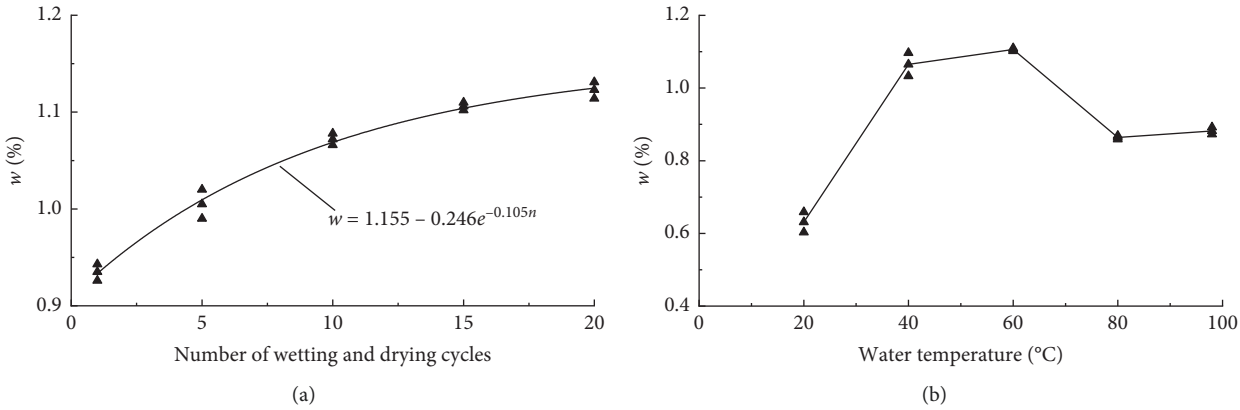

Figure 6: Water content variation after cyclic wetting and drying treatment. (a) Water content versus the number of wetting and drying cycles. (b) Water content versus water temperature.

enhanced by water temperature. There is a nonlinear relation between water content and water temperature. Water content increases with water temperature increasing from 20°C to 40°C. Water content at 60°C is slightly larger than that at 40°C. With water temperature increasing from 60°C to 80°C, water content decreases. Water content at 98°C is slightly bigger than that at 80°C.

3.2. P-Wave Velocity Variation during Cyclic Wetting and Drying Treatment. Before conducting dynamic uniaxial compressive tests, P-wave velocity of the wet sandstone specimen after cyclic wetting and drying treatment was measured by using an NM-4B nonmetallic ultrasonic detector. P-wave velocity test results are illustrated in Figure 7.

As illustrated in Figure 7(a), after 1 cycle of wetting and drying, P-wave velocity of the wet sandstone specimen increases due to open pores and microcracks filled with water. With continuous cyclic wetting and drying treatment, P-wave velocity decreases in an exponential function due to the initiation and propagation of microcracks.

Seen from Figure 7(b), P-wave velocity also fluctuates with water temperature in wetting process. Compared with the P-wave velocity at 20°C, elevating water temperature in wetting process leads to a decrease in P-wave velocity of the sandstone specimen after 15 cycles of wetting and drying treatment; in other words, the deterioration of P-wave velocity is accelerated by water temperature. There is also a nonlinear relation between P-wave velocity and water temperature. P-wave velocity reduces with water temperature increasing from 20°C to 60°C, and then it increases with water temperature increasing from 60°C to 80°C. P-wave velocity at 80°C is roughly the same with that at 98°C.

4. Dynamic Uniaxial Compressive Test Results and Analyses

4.1. Variation of Dynamic Uniaxial Compressive Characteristics versus Wetting and Drying Cycles. After cyclic wetting and drying treatments, sandstone specimens were put into a 20°C water bath for 4 hours to cool down. Based on the acquired incident, reflected, and transmitted stress waves in dynamic uniaxial compressive tests, dynamic characteristics of the wet sandstone specimen were derived based on three-wave methods [28]. In line with previous researches [4, 41, 46–48], dynamic elastic modulus was defined as the tangent modulus corresponding to 40% and 60% of dynamic uniaxial compressive strength during the rising phase of dynamic stress-strain curve. According to the ISRM suggested method [28], the average strain rate was determined by the flat region in the strain rate-time curve [23].

When water temperature in wetting process was 60°C, dynamic uniaxial compressive tests were carried out under the same impact air pressure, namely, the same loading condition. Test results of the wet sandstone specimen after cyclic wetting and drying treatment are illustrated in Figure 8. In Figure 8, WD is short for wetting and drying cycle and the following number represents the number of wetting and drying cycles. Without WD denotes the oven-dried sandstone specimen.

It is seen from Figure 8(a) that compared with the static compressive test result, no compaction stage is illustrated in dynamic stress-strain curves, which makes the prefailure region of dynamic stress-strain nearly linear. Moreover, dynamic uniaxial compressive strength and dynamic elastic modulus are much bigger than those in the static condition. Similar to the results in previous studies [22, 23], dynamic stress-strain curves of the wet sandstone specimen gradually go towards the down and the right with cyclic wetting and drying treatment, which implies that the deterioration induced by cyclic wetting and drying treatment makes the sandstone specimen more ductile to some extent. After 1 cycle of wetting and drying, dynamic compressive stress-strain curve of the wet sandstone specimen is a little bit higher than that of the oven-dried sandstone specimen, which is the results of viscous behavior of water, including the meniscus effect, Stefan effect, and Newton inner friction effect [22, 49, 50].

As illustrated in Figures 8(b) and 8(c), both dynamic uniaxial compressive strength and dynamic elastic modulus decrease in an exponential function with the increase of wetting and drying cycles. On the contrary, the average strain rate increases in an exponential function with the increase of wetting and drying cycles, which is shown in

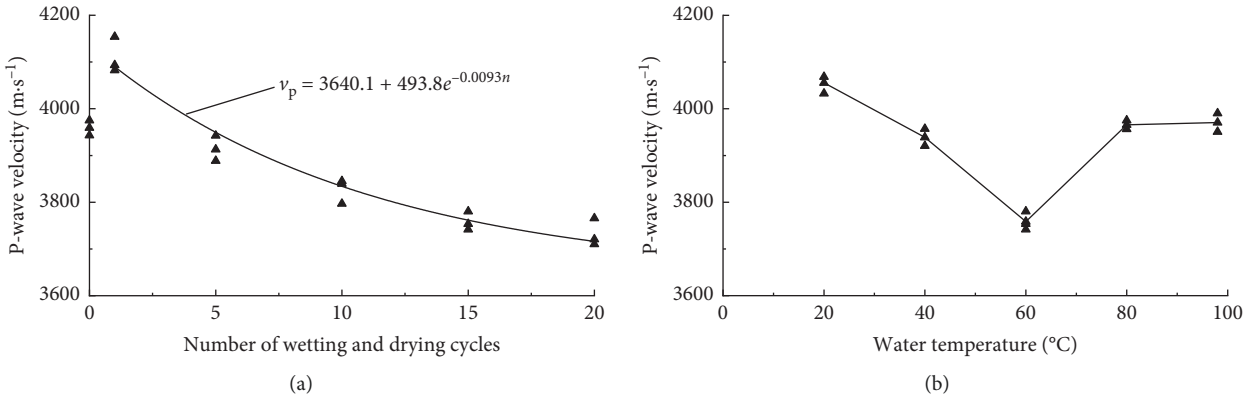

Figure 7: P-wave velocity variation after cyclic wetting and drying treatment. (a) P-wave velocity versus the number of wetting and drying cycles. (b) P-wave velocity versus water temperature.

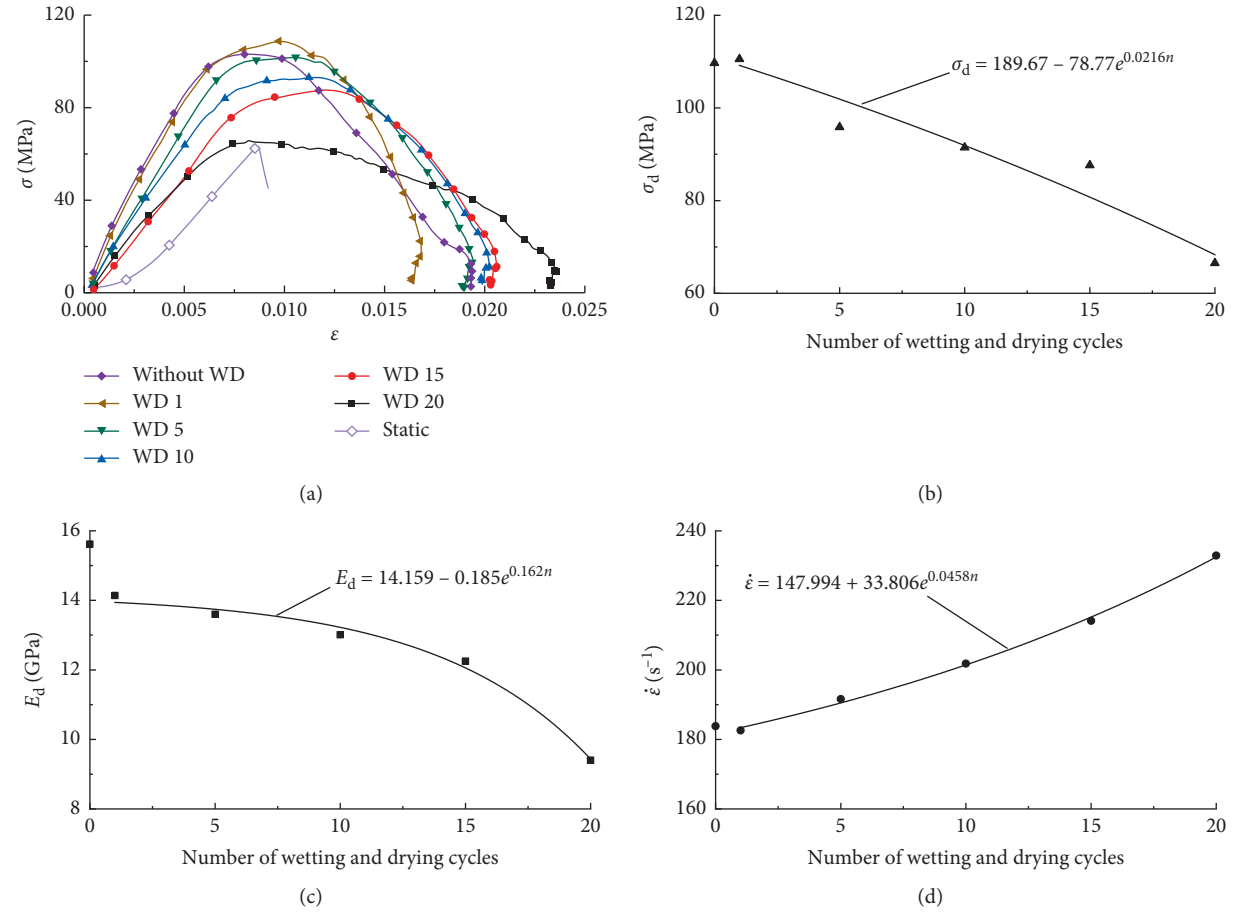

Figure 8: Dynamic uniaxial compressive characteristics variation versus wetting and drying cycles. (a) Dynamic compressive stress-strain curve. (b) Dynamic uniaxial compressive strength. (c) Dynamic elastic modulus. (d) Average strain rate.

Figure 8(d). Compared with dynamic uniaxial compressive strength after 1 cycle of wetting and drying, dynamic uniaxial compressive strength presents a 20.7% decrease after 15 cycles of wetting and drying and a 39.8% decrease after 20 cycles of wetting and drying. Similar to dynamic uniaxial compressive strength, the dynamic elastic modulus shows a 13.4% decrease after 15 cycles of wetting and drying and a 33.5% decrease after 20 cycles of wetting and drying. Reversely, the average strain rate displays a 17.2% increase after 15 cycles of wetting and drying and a 27.5% increase after 20

cycles of wetting and drying. Hence, an evident deterioration is shown when wetting and drying cycles increasing from 15 to 20.

4.2. Variation of Dynamic Uniaxial Compressive Characteristics versus Water Temperature. After 15 cycles of wetting and drying, the variation of dynamic compressive characteristics with water temperature in wetting process are shown in Figure 9.

Compared with dynamic stress-strain curve at a water temperature of 20°C, elevating water temperature in wetting process from 20°C to 98°C makes the dynamic stress-strain curve shift to the down and right, which is shown in Figure 9(a). In other words, the deterioration induced by cyclic wetting and drying is enhanced by elevating water temperature in wetting process, but the enhancement effect is nonlinear with water temperature in wetting process. Moreover, water temperature at 60°C demonstrates a prominent deterioration effect.

As illustrated in Figure 9(b), dynamic uniaxial compressive strength first decreases with water temperature increasing from 20°C to 60°C, and then it increases with water temperature increasing from 60°C to 80°C. Dynamic uniaxial compressive strength at 98°C is slightly smaller than that at 80°C. Dynamic uniaxial compressive strength at 60°C presents a 13.8% decrease compared with that at 20°C.

It is seen from Figure 9(c) that the dynamic elastic modulus first decreases with water temperature increasing from 20°C to 40°C and then it increases slightly from 40°C to 80°C and dramatically from 80°C to 98°C. Compared with the dynamic elastic modulus at 20°C, the dynamic elastic modulus presents a 21.4% decrease at 40°C and a 19.5% decrease at 60°C. The turning point of the dynamic elastic modulus is at 40°C and not at 60°C, and this may be the result of the transition at about 50% of dynamic compressive strength in the dynamic stress-strain curve at 40°C, which can be seen in Figure 9(a). The transition at 50% of dynamic compressive strength may be caused by the connection and propagation of some tiny microcracks induced by cyclic wetting and drying during the loading process.

As shown in Figure 9(d), the average strain rate first increases with water temperature increasing from 20°C to 60°C and then decreases from 60°C to 98°C. Average strain rate at 60°C demonstrates an 18.5% increase compared with that at 20°C.

4.3. Variation of Dynamic Fragments. To evaluate the fracture characteristic of sandstone, dynamic fragments of sandstone were sieved after dynamic uniaxial compressive tests. The size of involved sieves were 31.5 mm, 25 mm, 20 mm, 16 mm, 10 mm, 5 mm, 2.5 mm, 1.25 mm, and 0.63 mm. After sieving, average fragment size is used to describe the fracture degree and is calculated by using the following equation [51]:

$$d_s = \frac{\sum \eta_i d_i}{\sum \eta_i}, \tag{3}$$

where d_s represents average fragment size, d_i is the mean size of sandstone fragments in the sieve, and η_i is the mass percentage of sandstone fragments corresponding to d_i.

The variation of average fragment size after cyclic wetting and drying treatment is shown in Figure 10.

As illustrated in Figure 10(a), average fragment size decreases in an exponential function with the number of wetting and drying cycles, which indicates that cyclic wetting and drying treatment leads to small fragments. It is seen from Figure 10(b) that average fragment size first decreases and then increases with elevating water temperature from 20°C to 98°C. And average fragment size at 60°C is smaller than that at other water temperatures.

Based on fractal geometry, sandstone fragment distribution was evaluated by fractal dimension. Fractal dimension of sandstone fragments is derived by using the mass-equivalent dimension curve and is calculated by using the following equation [4, 52]:

$$D_f = 3 - \frac{\ln(m_i/M)}{\ln d_i}, \tag{4}$$

where D_f denotes the fractal dimension, M is the total mass of fragments, and m_i is the cumulative mass of fragments passing the sieve with a diameter of d_i.

Figure 11 shows the fractal dimension variation with the number of wetting and drying cycles and water temperature in wetting process.

As illustrated in Figure 11, fractal dimension variation is contrary to the variation of average fragment size. According to Figure 11(a), fractal dimension increases in an exponential function with the number of wetting and drying cycles. It is seen from Figure 11(b) that fractal dimension first increases and then decreases with elevating water temperature from 20°C to 98°C. Fractal dimension at 60°C is larger than that at other water temperatures.

4.4. Variation of Damage Evolution. Before dynamic uniaxial compressive tests, sandstone specimens have already been damaged by cyclic wetting and drying. Assuming the damage value of the wet sandstone specimen after 1 cycle of wetting and drying is zero, damage induced by cyclic wetting and drying is calculated by using P-wave velocity [4]:

$$D_{WD} = 1 - \left(\frac{v_n}{v_1}\right)^2, \tag{5}$$

where D_{WD} stands for the damage induced by cyclic wetting and drying, v_n is the P-wave velocity after n cycles of wetting and drying treatment, and v_1 is the P-wave velocity after 1 cycle of wetting and drying treatment.

Figure 12 shows the variation of damage induced by cyclic wetting and drying.

Figure 12(a) shows that damage induced by cyclic wetting and drying increases in an exponential function with the number of wetting and drying cycles, which implies a damage accumulation in continuous cyclic wetting and drying treatment. Figure 12(b) indicates that damage induced by cyclic wetting and drying first increases and then

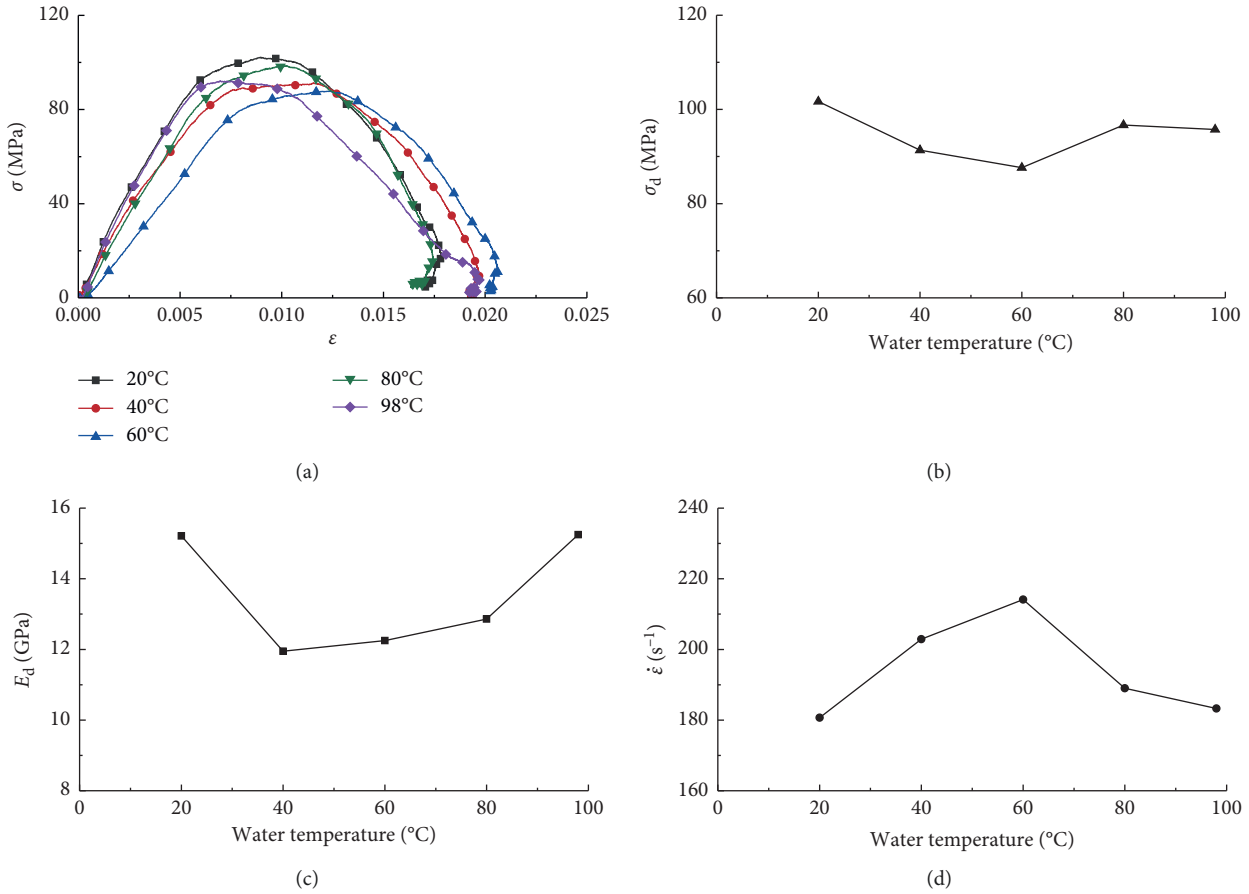

Figure 9: Dynamic uniaxial compressive characteristics variation versus water temperature. (a) Dynamic compressive stress-strain curve. (b) Dynamic uniaxial compressive strength. (c) Dynamic elastic modulus. (d) Average strain rate.

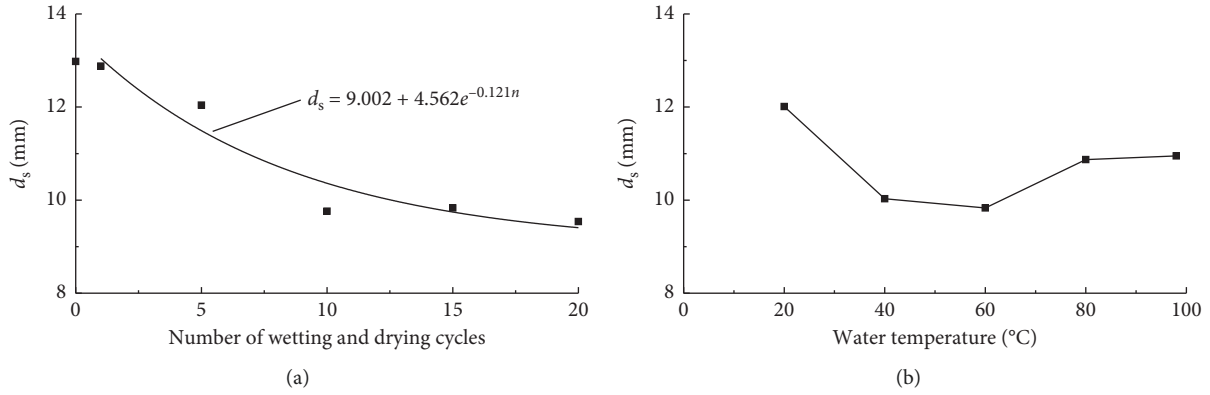

Figure 10: Average fragment size variation after cyclic wetting and drying treatment. (a) Average fragment size versus the number of wetting and drying cycles. (b) Average fragment size versus water temperature.

decreases with elevating water temperature from 20°C to 98°C. Damage induced by cyclic wetting and drying at 60°C is larger than that at other water temperatures.

As deformation and failure of rock is an irreversible process of energy dissipation [53], mechanical damage is considered as the ratio of dissipated energy to total absorbed energy and is calculated by using the following equation:

$$D_M = \frac{\int_0^{\varepsilon} \sigma d\varepsilon - (\sigma^2/2E_d)}{\int \sigma d\varepsilon}, \quad (6)$$

where D_M represents mechanical damage during the loading process, σ and ε denote the stress and strain values at a certain point in time during the loading process, E_d denotes

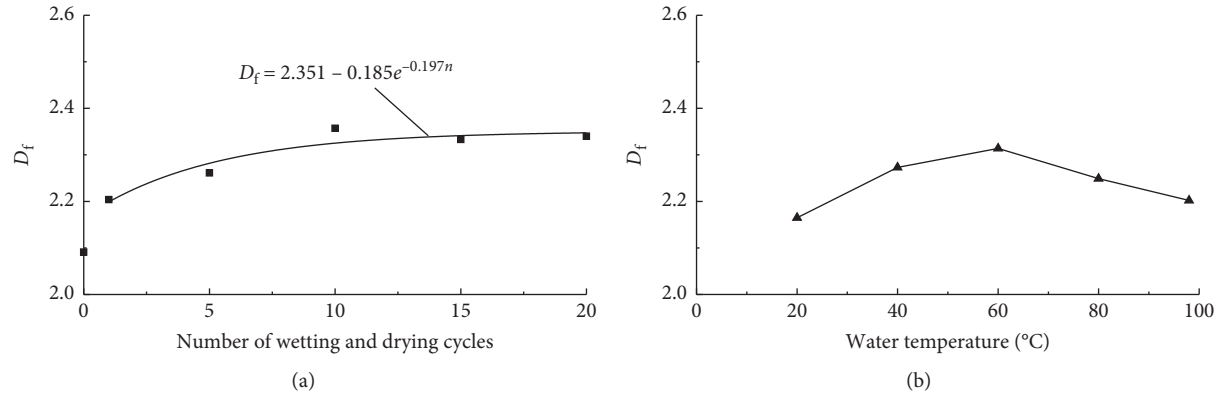

Figure 11: Fractal dimension variation after cyclic wetting and drying treatment. (a) Fractal dimension versus the number of wetting and drying cycles. (b) Fractal dimension versus water temperature.

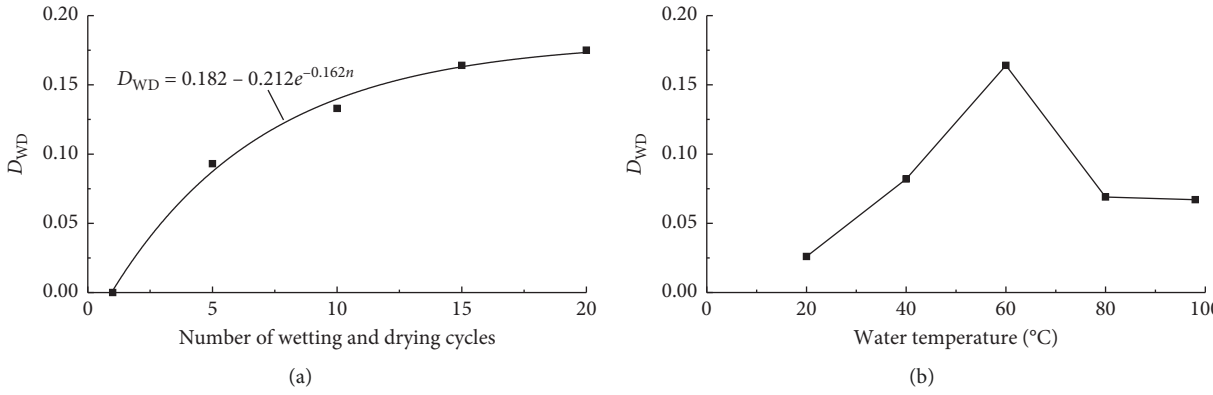

Figure 12: Variation of D_{WD} after cyclic wetting and drying treatment. (a) D_{WD} versus the number of wetting and drying cycles. (b) D_{WD} versus water temperature.

the dynamic elastic modulus during the loading process, $\int_0^\varepsilon \sigma d\varepsilon$ represents absorbed energy of a sandstone unit at a certain point in time during the loading process, and $\int \sigma d\varepsilon$ stands for total absorbed energy of a sandstone unit.

As sandstone specimens were already damaged by cyclic wetting and drying before dynamic uniaxial compressive tests, mechanical damage evolution is coupled with damage induced by cyclic wetting and drying. Coupling damage during the loading process can be calculated by using the following equation [54]:

$$D = 1 - (1 - D_{WD})(1 - D_M) = D_{WD} + (1 - D_{WD})D_M, \quad (7)$$

where D stands for the coupling damage during the loading process.

According to equation (7), coupling damage evolution curves of sandstone specimens after cyclic wetting and drying treatment are analyzed and drawn in Figure 13.

Clearly from Figure 13, coupling damage evolution curves mainly consist of two stages, steady stage and rapid growth stage [40]. Combined with dynamic stress-strain curves in Figures 8(a) and 9(a), the steady stage in total coupling damage evolution corresponds to the approximate linear compression stage in dynamic stress-strain curves. Closely followed by the steady stage, coupling damage grows rapidly during the plastic stage and failure stage in dynamic stress-strain curves.

It is seen from Figure 13(a) that cyclic wetting and drying treatment affects not only the initial damage values but also the damage evolution rules during the loading process. With the increase of wetting and drying cycles, coupling damage in the steady stage increases, while the increase rate of coupling damage in the rapid growth stage decreases.

As illustrated in Figure 13(b), water temperature in wetting process also affects the initial damage values and damage evolution rules during the loading process. With water temperature elevating from 20°C to 98°C, coupling damage in the steady stage first increases and then decreases, while the increase rate of coupling damage in the rapid growth stage first decreases and then increases. The turning point is also at 60°C.

5. Discussion

5.1. Effect of Cyclic Wetting and Drying. As discussed above, cyclic wetting and drying treatment has a detrimental effect on both physical and dynamic uniaxial compressive

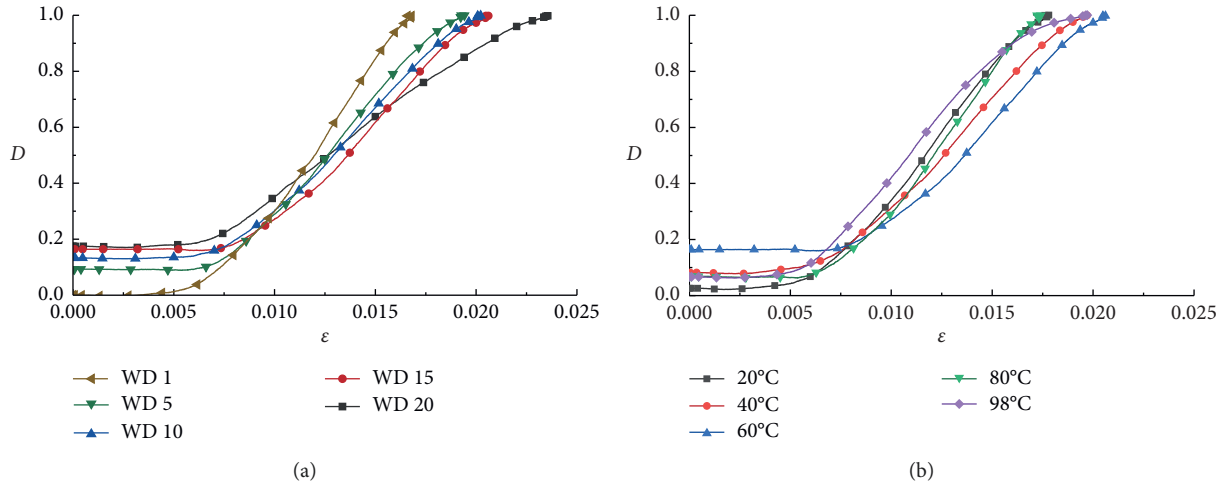

Figure 13: Coupling damage evolution during dynamic uniaxial compressive tests. (a) Coupling damage evolution after various wetting and drying cycles. (b) Coupling damage evolution under different water temperatures.

characteristics of sandstone. To evaluate the detrimental effect of cyclic wetting and drying, SEM technique was adopted to reveal the microscopic variation of sandstone after cyclic wetting and drying treatment. After dynamic uniaxial compressive tests, sandstone samples used for SEM observation were taken from relatively complete big fragments to eliminate the influence of the loading stress wave. SEM images were taken with a magnification ratio of 1000. When the temperature was 60°C in both wetting and drying processes, SEM images of the sandstone specimen subjected to different wetting and drying cycles are shown in Figure 14.

As illustrated in Figure 14(a), the original sandstone specimen is almost intact with barely any visible microcracks. After 5 cycles of wetting and drying treatment, newly generated microcracks marked with yellow circles are found in Figure 14(b). With continuous cyclic wetting and drying treatment, both the number and width of microcracks increase. After 20 cycles of wetting and drying, microcracks become more evident in Figure 14(e). Therefore, cyclic wetting and drying treatment leads to initiation and propagation of microcracks and induces damage in the sandstone specimen [23].

Generally, the detrimental effect of cyclic wetting and drying is a step by step process. Deterioration during cyclic wetting and drying is the result of the combined effect of physical and chemical damage and is closely associated with the mineral components of sandstone. Based on XRD analysis, tested sandstone contains lots of kaolinite. Kaolinite, a swelling clay mineral, brings out cyclic loading and unloading of tensile stresses within sandstone due to absorption and desorption of water during cyclic wetting and drying treatment. The cyclic loading and unloading of tensile stresses accelerate the growth and propagation of internal microcracks, as illustrated in Figure 14. Moreover, absorbed water in sandstone during wetting process has dissolving, erosion, and softening effects on rock minerals, which leads to unrecoverable deterioration on the cementation between rock grains [55]. As distilled water is used in wetting process, the hydrolysis of rock minerals can hardly occur. But soluble materials of sandstone dissolved in water still generate a few small hollows after a number of wetting and drying cycles. Therefore, both physical and dynamic uniaxial compressive characteristics deteriorate with the increase of wetting and drying cycles.

5.2. Effect of Water Temperature on Cyclic Wetting and Drying. After 15 cycles of wetting and drying treatment, SEM images of sandstone specimens in various water temperatures are shown in Figure 15. SEM images were taken with a magnification ratio of 10000.

Clearly from Figure 15, the micromorphology has been changed with elevating the water temperature in wetting process. With water temperature increasing from 20°C to 60°C, more microcracks generate, which implies that elevating water temperature can accelerate the damage induced by cyclic wetting and drying. While when water temperature continuously increases from 60°C to 98°C, the micromorphology is changed and fewer microcracks display, which is the result of kaolinite mobilization under high water temperature [56]. Microcracks are more evident at a water temperature of 60°C, which is consistent with the variation of damage induced by cyclic wetting and drying.

As only water temperature is changed in wetting process, the effect of water temperature on cyclic wetting and drying mainly focuses on the interaction between water and rock in wetting process. According to the previous studies [27, 57], there existed a threshold value for the influence of water temperature on the interaction between water and rock. When water temperature in wetting process was less than the threshold value, elevating the water temperature accelerated the interaction between water and rock. While when water temperature was beyond the threshold value, the interaction susceptibility to temperature decreased. Based on the variation of physical and dynamic uniaxial compressive properties of sandstone, the deterioration induced by cyclic

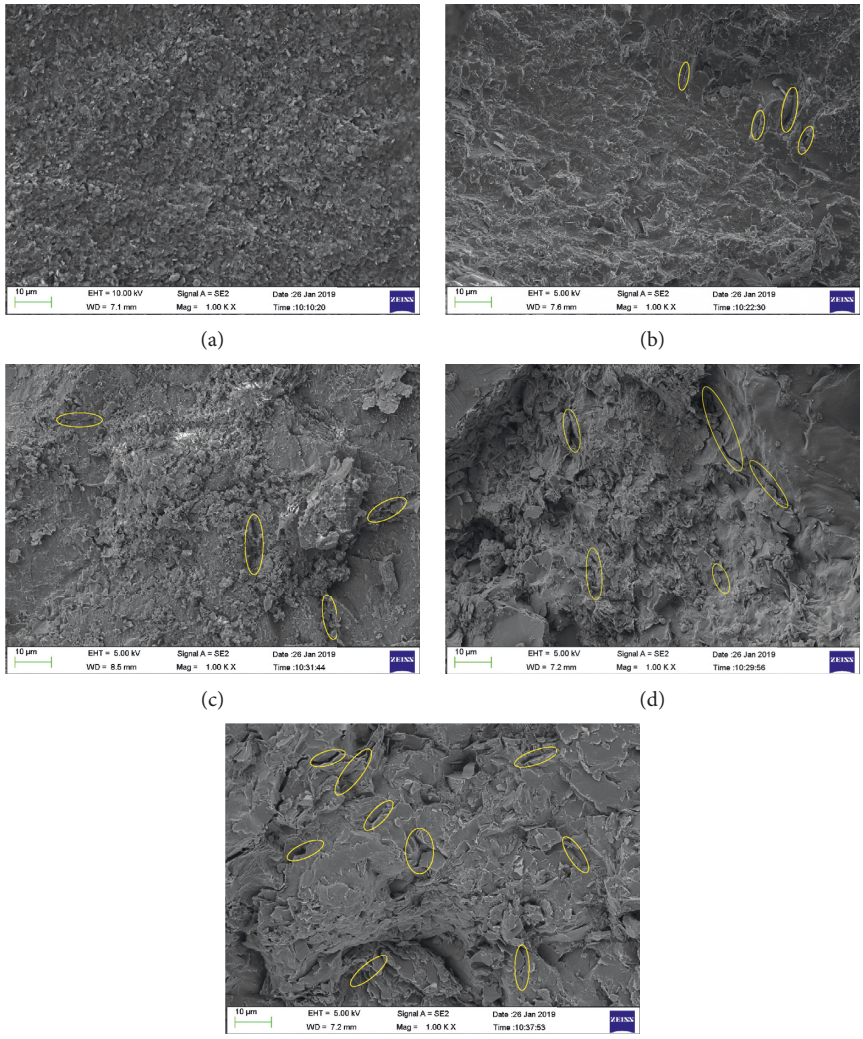

Figure 14: SEM images of the sandstone specimen after different wetting and drying cycles. (a) 0. (b) 5. (c) 10. (d) 15. (e) 20.

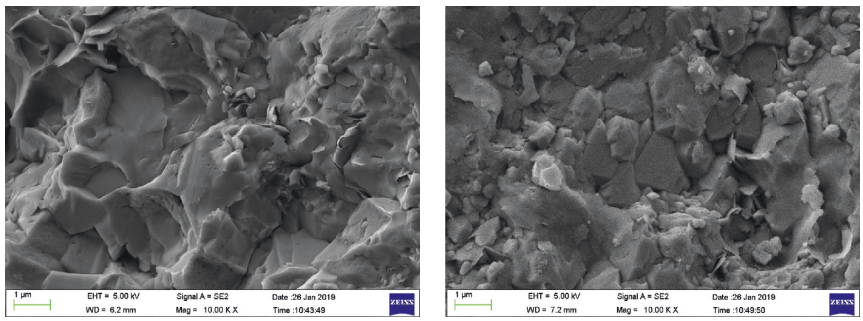

Figure 15: Continued.

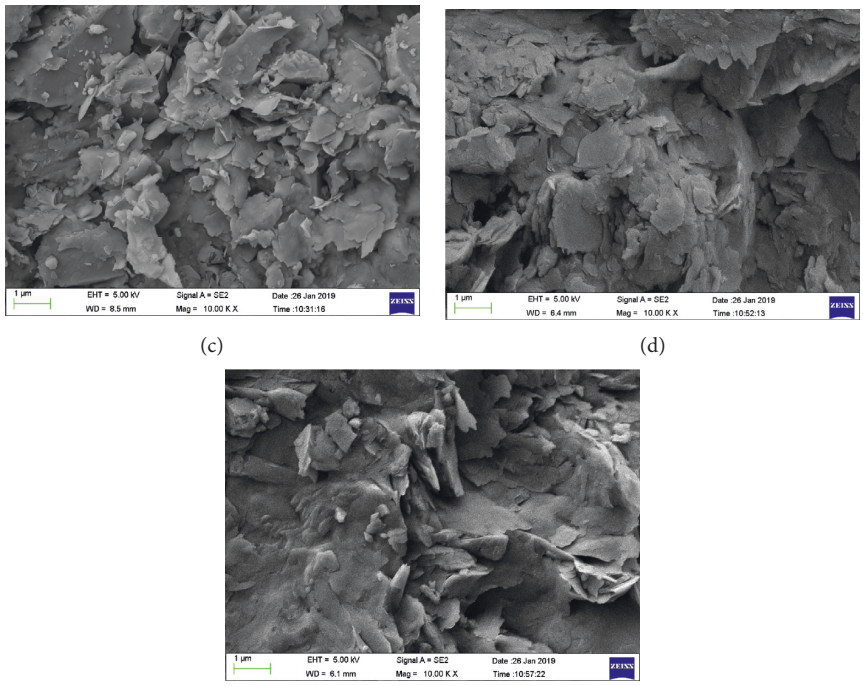

Figure 15: SEM images of the sandstone specimen after 15 cycles of wetting and drying in different water temperatures. (a) 20°C. (b) 40°C. (c) 60°C. (d) 80°C. (e) 98°C.

wetting and drying is accelerated nonlinearly with water temperature in wetting process. After 15 cycles of wetting and drying treatment, dynamic uniaxial compressive strength, dynamic elastic modulus, average fragment size, and P-wave velocity first decrease and then increase with elevating water temperature from 20°C to 98°C in wetting process, while average strain rate, fractal dimension, water content, and damage induced by cyclic wetting and drying first increase and then decrease with water temperature. The threshold value for the effect of water temperature on cyclic wetting and drying is found to be about 60°C for the tested sandstone. When water temperature in wetting process is less than 60°C, elevating the water temperature accelerates the deterioration induced by cyclic wetting and drying. On the contrary, when water temperature is beyond 60°C, the enhancement effect of water temperature on cyclic wetting and drying decreases with further elevating water temperature.

6. Conclusions

Based on dynamic uniaxial compressive tests, the combined effect of cyclic wetting and drying and water temperature on dynamic mechanical characteristics of sandstone was analyzed from the variation of dynamic uniaxial compressive strength, dynamic elastic modulus, average strain rate, fractal dimension, and damage evolution. Main conclusions are summarized as follows:

(1) SEM images indicate that cyclic wetting and drying treatment leads to the initiation and propagation of microcracks. As lots of kaolinite existed in sandstone, the initiation and propagation of microcracks is mainly caused by cyclic loading and unloading of tensile stresses during absorption and desorption of water in cyclic wetting and drying treatment.

(2) According to SEM images of sandstone after 15 cycles of wetting and drying treatment, more microcracks generate when water temperature in wetting process increases from 20°C to 60°C, while the micromorphology is changed and fewer microcracks display due to kaolinite mobilization when water temperature increases from 60°C to 98°C.

(3) Cyclic wetting and drying treatment demonstrates a detrimental effect on both physical and dynamic uniaxial compressive characteristics of sandstone. With the increase of wetting and drying cycles, dynamic compressive strength, dynamic elastic modulus, average fragment size, and P-wave velocity decrease in an exponential function, while average strain rate, fractal dimension, water content, and damage induced by cyclic wetting and drying increase in an exponential function.

(4) After 15 cycles of wetting and drying treatment, the deterioration of both physical and dynamic uniaxial compressive characteristics first increase and then decrease with water temperature in wetting process elevating from 20°C to 98°C. There is a threshold value for the effect of water temperature on cyclic wetting and drying, which is about 60°C for the tested sandstone. When water temperature in

wetting process is less than 60°C, elevating the water temperature accelerates the deterioration induced by cyclic wetting and drying. On the contrary, when water temperature is beyond 60°C, the enhancement effect of water temperature on cyclic wetting and drying treatment decreases with further elevating water temperature.

Data Availability

The data used to support the findings of this study are included within the article.

Conflicts of Interest

The authors declare that there are no conflicts of interest regarding the publication of this paper.

Acknowledgments

This research was funded by the Anhui Provincial Natural Science Foundation (no. 1808085QE148), project funded by China Postdoctoral Science Foundation (no. 2018M642504), Natural Science Research Project of Colleges and Universities in Anhui Province (no. KJ2017A097), Young Teacher Scientific Research Project of Anhui University of Science and Technology (no. QN201607), Doctoral Fund Project of Anhui University of Science and Technology (no. 11674), National Innovation and Entrepreneurship Training Program for College Students (no. 201810361029), and Anhui Provincial Innovation and Entrepreneurship Training Program for College Students (no. 201810361174).

References

[1] P. A. Hale and A. Shakoor, "A laboratory investigation of the effects of cyclic heating and cooling, wetting and drying, and freezing and thawing on the compressive strength of selected sandstones," *Environmental and Engineering Geoscience*, vol. 9, no. 2, pp. 117–130, 2003.

[2] M. Hu, Y. Liu, L. Song, and Y. Zhang, "Constitutive model and damage evolution of mudstone under the action of dry-wet cycles," *Advances in Civil Engineering*, vol. 2018, Article ID 9787429, 10 pages, 2018.

[3] M. H. Ghobadi and R. Babazadeh, "Experimental studies on the effects of cyclic freezing-thawing, salt crystallization, and thermal shock on the physical and mechanical characteristics of selected sandstones," *Rock Mechanics and Rock Engineering*, vol. 48, no. 3, pp. 1001–1016, 2015.

[4] R. R. Zhang and P. Yuan, "Effect of hydrothermal coupling on physical and dynamic mechanical properties of sandstone," *Advances in Civil Engineering*, vol. 2019, Article ID 7318768, 14 pages, 2019.

[5] Q. Jiang, F. Yan, J. Wu, Q. Fan, S. Li, and D. Xu, "Grading opening and shearing deformation of deep outward-dip shear belts inside high slope: a case study," *Engineering Geology*, vol. 250, pp. 113–129, 2019.

[6] Q. Jiang, G. Su, X. T. Feng, G. Chen, M. Z. Zhang, and C. Liu, "Excavation optimization and stability analysis for large underground caverns under high geostress: a case study of the Chinese Laxiwa project," *Rock Mechanics and Rock Engineering*, vol. 52, no. 3, pp. 895–915, 2019.

[7] D. Ma, H. Duan, X. Li, Z. Li, Z. Zhou, and T. Li, "Effects of seepage-induced erosion on nonlinear hydraulic properties of broken red sandstones," *Tunnelling and Underground Space Technology*, vol. 91, Article ID 102993, 2019.

[8] D. Ma, X. Cai, Q. Li, and H. Duan, "In-situ and numerical investigation of groundwater inrush hazard from grouted karst collapse pillar in longwall mining," *Water*, vol. 10, no. 9, p. 1187, 2018.

[9] D. Ma, H. Duan, J. Liu, X. Li, and Z. Zhou, "The role of gangue on the mitigation of mining-induced hazards and environmental pollution: an experimental investigation," *Science of the Total Environment*, vol. 664, pp. 436–448, 2019.

[10] Q. Y. Ma, P. Y. Yu, and P. Yuan, "Experimental study on creep properties of deep siltstone under cyclic wetting and drying," *Chinese Journal of Rock Mechanics and Engineering*, vol. 37, no. 3, pp. 593–600, 2018.

[11] B. Du, H. Bai, and G. Wu, "Dynamic compression properties and deterioration of red-sandstone subject to cyclic wet-dry treatment," *Advances in Civil Engineering*, vol. 2019, Article ID 1487156, 10 pages, 2019.

[12] G. Pardini, G. V. Guidi, R. Pini, D. Regüés, and F. Gallart, "Structure and porosity of smectitic mudrocks as affected by experimental wetting-drying cycles and freezing-thawing cycles," *Catena*, vol. 27, no. 3-4, pp. 149–165, 1996.

[13] A. Özbek, "Investigation of the effects of wetting-drying and freezing-thawing cycles on some physical and mechanical properties of selected ignimbrites," *Bulletin of Engineering Geology and the Environment*, vol. 73, no. 2, pp. 595–609, 2014.

[14] C. Gökceoğlu, R. Ulusay, and H. Sönmez, "Factors affecting the durability of selected weak and clay-bearing rocks from Turkey, with particular emphasis on the influence of the number of drying and wetting cycles," *Engineering Geology*, vol. 57, no. 3-4, pp. 215–237, 2000.

[15] Z. Zhao, J. Yang, D. Zhang, and H. Peng, "Effects of wetting and cyclic wetting-drying on tensile strength of sandstone with a low clay mineral content," *Rock Mechanics and Rock Engineering*, vol. 50, no. 2, pp. 485–491, 2017.

[16] H. Y. Yao, Z. H. Zhang, C. H. Zhu, Y. C. Shi, and Y. Li, "Experimental study of mechanical properties of sandstone under cyclic drying and wetting," *Rock and Soil Mechanics*, vol. 31, no. 12, pp. 3704–3708, 2010.

[17] X. R. Liu, D. L. Li, L. Zhang, and Z. Wang, "Influence of wetting-drying cycles on mechanical properties and microstructure of shaly sandstone," *Chinese Journal of Geotechnical Engineering*, vol. 38, no. 7, pp. 1291–1300, 2016.

[18] B. Y. Zhang, J. H. Zhang, and G. L. Sun, "Deformation and shear strength of rockfill materials composed of soft siltstones subjected to stress, cyclical drying/wetting and temperature variations," *Engineering Geology*, vol. 190, pp. 87–97, 2015.

[19] W. Hua, S. Dong, Y. Li, and Q. Wang, "Effect of cyclic wetting and drying on the pure mode II fracture toughness of sandstone," *Engineering Fracture Mechanics*, vol. 153, pp. 143–150, 2016.

[20] T. R. Stacey, "Addressing the consequences of dynamic rock failure in underground excavations," *Rock Mechanics and Rock Engineering*, vol. 49, no. 10, pp. 4091–4101, 2016.

[21] Q. B. Zhang and J. Zhao, "A review of dynamic experimental techniques and mechanical behaviour of rock materials," *Rock Mechanics and Rock Engineering*, vol. 47, no. 4, pp. 1411–1478, 2014.

[22] P. Yuan and Q. Y. Ma, "Split Hopkinson pressure bar tests on sandstone in coalmine under cyclic wetting and drying," *Rock and Soil Mechanics*, vol. 34, no. 9, pp. 2557–2562, 2013.

[23] Z. Zhou, X. Cai, L. Chen, W. Cao, Y. Zhao, and C. Xiong, "Influence of cyclic wetting and drying on physical and dynamic compressive properties of sandstone," *Engineering Geology*, vol. 220, pp. 1–12, 2017.

[24] Z. Zhou, X. Cai, D. Ma, L. Chen, S. Wang, and L. Tan, "Dynamic tensile properties of sandstone subjected to wetting and drying cycles," *Construction and Building Materials*, vol. 182, pp. 215–232, 2018.

[25] M. C. He and Y. P. Guo, "Deep rock mass thermodynamic effect and temperature control measures," *Chinese Journal of Rock Mechanics and Engineering*, vol. 32, no. 12, pp. 2377–2392, 2013.

[26] H. Fu, J. Chen, L. Zeng, and X. Qiu, "Experiment on the effects of temperature and humidity on uniaxial mechanical properties of silty mudstone," *China Civil Engineering Journal*, vol. 52, no. 1, pp. 89–98, 2019.

[27] P. Cao, G. Ning, X. Fan, H. Mei, and X. Huang, "Influence of water-rock interaction on morphological characteristic of rock joint surface at different temperatures," *Journal of Central South University (Science and Technology)*, vol. 44, no. 4, pp. 1510–1516, 2013.

[28] Y. X. Zhou, K. Xia, X. B. Li et al., "Suggested methods for determining the dynamic strength parameters and mode-I fracture toughness of rock materials," *International Journal of Rock Mechanics and Mining Sciences*, vol. 49, pp. 105–112, 2012.

[29] P. Yuan and Q. Y. Ma, "Correction of non-parallel end-faces of rock specimen in SHPB tests," *Explosion and Shock Waves*, vol. 37, no. 5, pp. 929–936, 2017.

[30] G. Khanlari and Y. Abdilor, "Influence of wet-dry, freeze-thaw, and heat-cool cycles on the physical and mechanical properties of upper red sandstones in central Iran," *Bulletin of Engineering Geology and the Environment*, vol. 74, no. 4, pp. 1287–1300, 2015.

[31] X. Liu, Z. Wang, Y. Fu, W. Yuan, and L. Miao, "Macro/microtesting and damage and degradation of sandstones under dry-wet cycles," *Advances in Materials Science and Engineering*, vol. 2016, Article ID 7013032, 16 pages, 2016.

[32] Z. Zhang, Q. Jiang, C. Zhou, and X. Liu, "Strength and failure characteristics of Jurassic red-bed sandstone under cyclic wetting-drying conditions," *Geophysical Journal International*, vol. 198, no. 2, pp. 1034–1044, 2014.

[33] H. F. Deng, J. L. Li, M. Zhu, K. W. Wang, L. H. Wang, and C. J. Deng, "Experimental research on strength deterioration rules of sandstone under "saturation-air dry" circulation function," *Rock and Soil Mechanics*, vol. 33, no. 11, pp. 3306–3312, 2012.

[34] Z. L. Zhou, L. Hong, Q. Y. Li, and Z. X. Liu, "Calibration of split Hopkinson pressure bar system with special shape striker," *Journal of Central South University of Technology*, vol. 18, no. 4, pp. 1139–1143, 2011.

[35] P. Yuan, Q. Y. Ma, and D. D. Ma, "Stress uniformity analyses on nonparallel end-surface rock specimen during loading process in SHPB tests," *Advances in Civil Engineering*, vol. 2018, Article ID 5406931, 12 pages, 2018.

[36] K. Xia and W. Yao, "Dynamic rock tests using split Hopkinson (Kolsky) bar system-a review," *Journal of Rock Mechanics and Geotechnical Engineering*, vol. 7, no. 1, pp. 27–59, 2015.

[37] Z. Zhou, X. Li, A. Liu, and Y. Zou, "Stress uniformity of split Hopkinson pressure bar under half-sine wave loads," *International Journal of Rock Mechanics and Mining Sciences*, vol. 48, no. 4, pp. 697–701, 2011.

[38] F. Dai, S. Huang, K. Xia, and Z. Tan, "Some fundamental issues in dynamic compression and tension tests of rocks using split Hopkinson pressure bar," *Rock Mechanics and Rock Engineering*, vol. 43, no. 6, pp. 657–666, 2010.

[39] P. Baranowski, J. Malachowski, R. Gieleta, K. Damaziak, L. Mazurkiewicz, and D. Kolodziejczyk, "Numerical study for determination of pulse shaping design variables in SHPB apparatus," *Bulletin of the Polish Academy of Sciences: Technical Sciences*, vol. 61, no. 2, pp. 459–466, 2013.

[40] P. Yuan, N. N. Wei, and Q. Y. Ma, "Effect of nonparallel end face on energy dissipation analyses of rocklike materials based on SHPB tests," *Shock and Vibration*, vol. 2019, Article ID 2040947, 11 pages, 2019.

[41] G. Li, L. Yu, H. Jing, H. Su, T. Zhang, and M. Li, "Experimental study of dynamic compressive mechanical properties of limestone after acid corrosion," *Rock and Soil Engineering*, vol. 38, no. 11, pp. 3247–3254, 2017.

[42] L. Hong, X. Li, X. Liu, Z. Zhou, Z. Ye, and T. Yin, "Stress uniformity process of specimens in SHPB test under different loading conditions of rectangular and half-sine input waves," *Transactions of Tianjin University*, vol. 14, no. 6, pp. 450–456, 2008.

[43] J. Zhu, S. Hu, and L. Wang, "An analysis of stress uniformity for concrete-like specimens during SHPB tests," *International Journal of Impact Engineering*, vol. 36, no. 1, pp. 61–72, 2009.

[44] L. N. Y. Wong, V. Maruvanchery, and G. Liu, "Water effects on rock strength and stiffness degradation," *Acta Geotechnica*, vol. 11, no. 4, pp. 713–737, 2016.

[45] J. A. Franklin, "Suggested methods for determining water-content, porosity, density, absorption and related properties and swelling and slake-durability index properties," *International Journal of Rock Mechanics and Mining Sciences*, vol. 16, no. 2, pp. 151–156, 1979.

[46] T. B. Yin, R. H. Shu, X. B. Li, P. Wang, and X. L. Liu, "Comparison of mechanical properties in high temperature and thermal treatment granite," *Transactions of Nonferrous Metals Society of China*, vol. 26, no. 7, pp. 1926–1937, 2016.

[47] B. Du and H. Bai, "A damage constitutive model of red sandstone under coupling of wet-dry cycles and impact load," *Shock and Vibration*, vol. 2019, Article ID 7692424, 12 pages, 2019.

[48] S. Liu and J. Xu, "Study on dynamic characteristics of marble under impact loading and high temperature," *International Journal of Rock Mechanics and Mining Sciences*, vol. 62, pp. 51–58, 2013.

[49] P. Yuan and R. Q. Ma, "Split Hopkinson pressure bar tests and analysis of coalmine sandstone with various moisture contents," *Chinese Journal of Rock Mechanics and Engineering*, vol. 34, no. s1, pp. 2888–2893, 2015.

[50] Z. Zhou, X. Cai, D. Ma et al., "Water saturation effects on dynamic fracture behavior of sandstone," *International Journal of Rock Mechanics and Mining Sciences*, vol. 114, pp. 46–61, 2019.

[51] L. Hong, Z. L. Zhou, T. B. Yin, G. Y. Liao, and Z. Y. Ye, "Energy consumption in rock fragmentation at intermediate strain rate," *Journal of Central South University of Technology*, vol. 16, no. 4, pp. 677–682, 2009.

[52] A. Lu, S. Hu, M. Li, T. Duan, B. Li, and X. Chang, "Impact of moisture content on the dynamic failure energy dissipation characteristics of sandstone," *Shock and Vibration*, vol. 2019, Article ID 6078342, 10 pages, 2019.

[53] H. P. Xie, R. D. Peng, Y. Ju, and H. W. Zhou, "Energy analysis of rock failure," *Chinese Journal of Rock Mechanics and Engineering*, vol. 24, no. 15, pp. 2603–2608, 2005.

[54] P. Wang, J. Xu, X. Fang, and P. Wang, "Energy dissipation and damage evolution analyses for the dynamic compression failure process of red-sandstone after freeze-thaw cycles," *Engineering Geology*, vol. 221, pp. 104–113, 2017.

[55] Z. Zhou, X. Cai, D. Ma, W. Cao, L. Chen, and J. Zhou, "Effects of water content on fracture and mechanical behavior of sandstone with a low clay mineral content," *Engineering Fracture Mechanics*, vol. 193, pp. 47–65, 2018.

[56] E. Rosenbrand, I. L. Fabricius, and H. Yuan, "Thermally induced permeability reduction due to particle migration in sandstones: the effect of temperature on kaolinite mobilisation and aggregation," in *Proceedings of the Thirty-Seventh Workshop on Geothermal Reservoir Engineering*, Stanford University, Stanford, CA, USA, January-February 2012.

[57] X. S. Zhou, X. Lv, and X. X. Liu, "Experimental study on failure process characteristic of considered about the water-temperature of argillaceous siltstone," *China Mining Magazine*, vol. 25, no. 5, pp. 141–145, 2016.